Cortical and Cytoplasmic Flow Polarity in Early Embryonic Cells of *Caenorhabditis elegans*

Steven N. Hird and John G. White

Medical Research Council Laboratory of Molecular Biology, Hills Road, Cambridge, CB2 2QH, England

Abstract. We have examined the cortex of *Caenorhabditis elegans* eggs during pseudocleavage (PC), a period of the first cell cycle which is important for the generation of asymmetry at first cleavage (Strome, S. 1989. *Int. Rev. Cytol.* 114: 81–123). We have found that directed, actin dependent, cytoplasmic, and cortical flow occurs during this period coincident with a rearrangement of the cortical actin cytoskeleton (Strome, S. 1986. *J. Cell Biol.* 103: 2241–2252). The flow velocity (4–7 μm/min) is similar to previously determined particle movements driven by cortical actin flows in motile cells. We show that directed flows occur in one of the daughters of the first division that itself divides asymmetrically, but not in its sister that divides symmetrically. The cortical and cytoplasmic events of PC can be mimicked in other cells during cytokinesis by displacing the mitotic apparatus with the microtubule polymerization inhibitor nocodazole. In all cases, the polarity of the resulting cortical and cytoplasmic flows correlates with the position of the attenuated mitotic spindle formed. These cortical flows are also accompanied by a change in the distribution of the cortical actin network. The polarity of this redistribution is similarly correlated with the location of the attenuated spindle. These observations suggest a mechanism for generating polarized flows of cytoplasmic and cortical material during embryonic cleavages. We present a model for the events of PC and suggest how the poles of the mitotic spindle mediate the formation of the contractile ring during cytokinesis in *C. elegans*.

THE phenomenon of cortical flow has been described in many systems including the lamellipodia of motile cells (Abercrombie et al., 1970; Heath, 1983; Fisher et al., 1988), the growth cones of neurons (Forscher and Smith, 1990), during amoeboid locomotion (Grebecki, 1984), and during cytokinesis (Dan, 1954). In these cases, material adjacent to the plasma membrane flows in a continual and directed manner away from one region to a distant region. For example, in the case of motile cells, patches of aggregated membrane proteins (Taylor et al., 1971; Holifield and Jacobson, 1991), or particles (Abercrombie et al., 1970; Fisher et al., 1988) applied to the dorsal surface of the lamellipodia, flow away from the leading edge of the cell. There is now significant evidence, derived from a number of observations, that there is continual movement of the underlying cortical actin network (Heath, 1983; Wang, 1985; Forscher and Smith, 1988) in motile cells. Membrane proteins may be associated with such moving cortical networks and so may be swept along in the same direction (Holifield et al., 1990), and they may in turn carry along extracellular particles. Alternative hypotheses predict that the cortical flows are driven by flows of membrane lipid (Bretscher, 1976, 1984). Although it has been suggested that this type of flow is not solely responsible for cortical flow during capping (Sheetz et al., 1989; Lee et al., 1990; Kucik et al., 1990), it is still possible that it may contribute to cortical movements.

There is a period in the first cell cycle of the *Caenorhabditis elegans* embryo during which a number of cytoskeletal and cytoplasmic rearrangements occur which bear some similarities to the cortical flows seen in other organisms. During the interval known as pseudocleavage (PC)[1] the anterior cortex of the fertilized egg undergoes a series of contractions; cytoplasm flows towards the posterior end of the egg and a transient cleavage furrow (the pseudocleavage furrow) forms and then regresses (Nigon, 1960). It is believed that at least some of these events are crucial for the correct partitioning of developmental determinants in the egg (Hill and Strome, 1988, 1990; Strome, 1989; Kirby et al., 1990). In particular, the cytoplasmic flow could carry determinants to the posterior end of the egg in a nonspecific way where they could then be anchored before the first determinative cleavage. Germ-line specific granules (P granules), may be localized to the posterior periphery of the egg in this way (Strome and Wood, 1982). There is a striking reorganization of the cortical actin network concomitant with the events of

Please address all correspondence to S. N. Hird, Medical Research Council Laboratory of Molecular Biology, Hills Road, Cambridge, CB2 2QH, England.

1. *Abbreviations used in this paper*: MA, mitotic apparatus, PC, pseudocleavage.

PC (Strome, 1986). Initially, actin fibers and foci are uniformly distributed throughout the egg cortex, but the foci become progressively concentrated in the anterior cortex. There is also immunocytological evidence that cortical myosin is redistributed similarly at this time (Strome, S., personal communication). It has therefore been suggested that during PC, cortical actin and, possibly, myosin form a contractile network that becomes localized to the anterior cortex displacing cytoplasm (and determinants) posteriorly (Strome, 1989). We are interested in understanding how this fundamental reorganization of the egg cortex is brought about, as it may reveal how the polarity of an asymmetric cleavage is determined.

In this paper we show that there is a directed flow of cortical material during PC in *C. elegans* by using a time lapse microscopy system that records multiple focal levels. We show that there is a similar cortical flow before cleavage in another blastomere which partitions cytoplasmic components before division but no directed flow in its sister which subsequently divides symmetrically. Furthermore, the cytoplasmic and cortical flows of PC, the formation of the transient furrow and the accumulation of cortical actin can be mimicked in other blastomeres during cytokinesis by treatment with the microtubule polymerization inhibitor nocodazole. This drug reduces the size of the mitotic spindle and often causes it to lie close to the cell cortex. In all cases, the orientation of the flows and the site of the accumulation of cortical actin are correlated with the location of the mitotic spindle. This suggests a general mechanism for generating directed flows of cytoplasm.

Materials and Methods

Nematode Culture

Wild type (N2) *Caenorhabditis elegans* strain Bristol was cultured on agar plates at 20°C with *Escherichia coli* strain OP50 as a food source (Brenner, 1974). Embryos were obtained from young gravid adults by dissection into egg salts (118 mM NaCl, 40 mM KCl, 3.4 mM $MgCl_2$, 3.4 mM $CaCl_2$, 5 mM Hepes, pH 7.4; Edgar and McGhee, 1986). Early embryos were identified using a dissecting microscope, and then grouped together using the tip of a scalpel blade. They were moved for observation using a drawn out capillary tube. Embryos which had completed the second meiotic division before dissection survived this procedure; those isolated before the completion of meiosis usually arrested.

Observation of Embryos

Embryos were deposited onto a glass coverslip coated with a solution of 0.1% polylysine (Sigma Chem. Co., St. Louis, MO). The coverslip was then inverted over a depression slide containing egg salts. The embryos were observed using a Zeiss Axioplan microscope equipped with Nomarski differential interference optics and a Hamamatsu C2400 video camera with analogue black-level subtraction. A time-lapse microscopy system was used to record events taking place on the surface and in the cytoplasm simultaneously (see below).

Multiple Focal Plane Time-Lapse Recording System

A system was developed that allows a user to make time-lapse recordings of multiple focal planes, allowing three-dimensional events to be followed in time. The system uses a Sony LVR-LVS/6000 optical disk system controlled via a serial link from a lap-top computer. The computer is also used to control a motorized focus drive unit (as used in a BioRad MRC 500/600 confocal microscope) by means of a second serial port. The software system allows the user to specify the number of focal planes per scan, the separation between planes, the time interval between focus scans, the total number of focus scans and a file name for referencing the data on playback. All the parameters of a recording run are stored on a dedicated digital area on the video disk, and a directory may be obtained of all the video "files" existing on the currently mounted disk cartridge. When recording, a single video frame is captured and recorded at each focal level in a scan; scans are repeated at the specified intervals. On playback a user can replay the recording forwards and backwards in time at a specified focal level or go up and down through the focal levels at a given point in time. In this way it is possible to track objects in three dimensions over the period in which the recording was made. The programs were written by Mike Thomson of the Laboratory of Molecular Biology Electronics Workshop.

Treatment of Embryos with Inhibitors

As early pronuclear stage embryos are permeable to nocodazole, treatment of these embryos with this drug was accomplished by using the appropriate concentration of nocodazole (from a 5 mg/ml in DMSO stock solution) in egg salts. Older embryos were treated by laser permeabilizing the chitinous eggshell in the presence of egg salts containing nocodazole. Embryos were also permeabilized to cytochalasin D (from a 1 mg/ml in DMSO stock solution) using the laser. Laser microbeam permeabilization was performed as described previously (Hyman and White, 1987).

Surface and Cytoplasmic Granule Tracing

Granules were traced directly from the video monitor onto acetate sheets at suitable time intervals.

Microfilament Staining

Partially synchronized young adults were washed from NGM plates into M9 buffer (Brenner, 1974). The worms were treated with 3% hypochlorite, 0.8 M NaOH in M9 which causes them to break open and release their embryos. The embryos were collected by centrifugation in a benchtop centrifuge (1,500 rpm, 30 s). The embryos were washed twice in M9 with centrifugation, and then resuspended in 10 μg/ml nocodazole in egg salts. The resuspended embryos were then permeabilized by being forced with moderate pressure through a 30 g needle to remove the eggshells. The permeabilized embryos were incubated for ~5–10 min at room temperature in the nocodazole solution. Microfilament fixation and staining was performed as described in Hill and Strome (1988). To fix, an equal volume of freshly prepared 3.0% paraformaldehyde, 0.2% glutaraldehye in egg salts was added and mixed quickly. Only permeabilized embryos were fixed by this procedure; such embryos would have therefore been permeable to the nocodazole. Fixation was allowed to proceed for 3 h at 16°C with shaking. After fixation, the embryos were collected by centrifugation, resuspended in a solution of 0.5% Triton X-100 in egg salts, and extracted for 1 h at room temperature. The embryos were collected by centrifugation and resuspended in 6.6 nM Bodipy- phallacidin (Molecular Probes Inc., Eugene, OR) in PBS containing 0.25% Triton X-100. They were then stained overnight at 16°C with agitation. The stained embryos were collected by centrifugation, resuspended in a small volume of PBS containing 1 μg/ml DAPI to stain the nuclei, and placed on a polylysine-coated slide. A coverslip with two greased edges was laid over the embryos, and PBS was wicked underneath to wash. Finally, the embryos were mounted in DABCO/glycerol and examined using a BioRad MRC-600 laser-scanning confocal microscope.

Summary of the Early Events in C. elegans Embryogenesis

The early stages of *C. elegans* embryogenesis have been described previously (Nigon, 1960; Hirsh et al., 1976) but will be reiterated here to aid interpretation of the data. *C. elegans* oocytes are arrested in prophase of meiosis. When visualized by Nomarski optics, embryos appear to be densely packed with granules. These are phase irregularities ~700 nm in diameter. Fertilization by the sperm occurs at what will become the posterior end of the embryo (it is not known if this is the result of a preexisting anteroposterior polarity or if the sperm entry actually defines the posterior end). As well as the paternal chromosome set, the sperm pronucleus brings the microtubule organizing center (centrosome) into the ooctye. Meiosis resumes after fertilization, and two polar bodies are extruded from the anterior end of the embryo. The single sperm centrosome duplicates, and then the two migrate until they are diametrically opposed to each other on an axis transverse to the anterior posterior axis (Hyman and White, 1987). At this point, the pronuclei start to become visible at the poles of the egg, and PC begins as described above. During PC, the an-

terior cortex exhibits ruffling activity and the PC furrow forms (see Fig. 1 *A*). This furrow is unusual in that it does not bisect a mitotic spindle. The oocyte pronucleus begins to migrate from the anterior end of the egg towards the sperm pronucleus at the posterior end (Albertson, 1984). Simultaneously, there is a flow of cytoplasmic material from anterior to posterior (Nigon, 1960) that stops by the time the maternal pronucleus migrates through the PC furrow (see Fig. 1 *B*). The sperm pronucleus begins to move off the posterior cortex to meet the oocyte pronucleus. After the meeting of the pronuclei in the posterior, the PC furrow relaxes, and cortical activity ceases (see Fig. 1 *C*).

Germ-line specific granules, termed P granules, become redistributed during PC. Initially they are uniformly distributed in the egg, but they coalesce and become progressively concentrated in the posterior of the egg as PC proceeds (Strome and Wood, 1982). Although the function of P granules is unknown, they serve as a useful model for the behavior of localized determinants.

The mitotic spindle is then set up along the anterior-posterior axis (see Fig. 1, *D–F*). The spindle becomes asymmetrically placed as it elongates, such that the posterior aster (centrosomes and microtubules) is closer to an end of the embryo than the anterior aster (see Fig. 1 *F*). This first division is asymmetric and determinative. It produces the larger anterior daughter AB and the smaller posterior daughter P_1 (see Fig. 1 *G*). The P_1 blastomere inherits all the P granules (Strome and Wood, 1982).

After first cleavage, the nucleus in P_1 migrates posteriorly while its centrosome duplicates (see Fig. 1 *H*). The centrosome inherited by AB duplicates after the centrosome in P_1 (Hyman and White, 1987).

The spindle in AB is set up along the dorsal-ventral axis orthogonal to the first anterior-posterior spindle axis (see Fig. 1, *J* and *K*). The AB division is equal and proliferative (Priess and Thomson, 1987). The P_1 spindle is set up along the anterior-posterior axis (see Fig. 1 *K*) and becomes asymmetrically placed as in P_0. Nuclear membrane breakdown and cytokinesis in P_1 begin 2 min after the same events in AB. The unequal, determinative division of P_1 produces the larger anterior daughter EMS and the smaller posterior daughter P_2 that inherits the P granules (Sulston et al., 1983; Strome and Wood, 1982) (see Fig. 1 *L*).

Results

Flow of Granules Near the Cortex of the Egg during Pseudocleavage

A summary of early embryogenesis in *C. elegans* is presented in Fig. 1 (see Materials and Methods for details). We visualized the events that occur in the cortex (subjacent

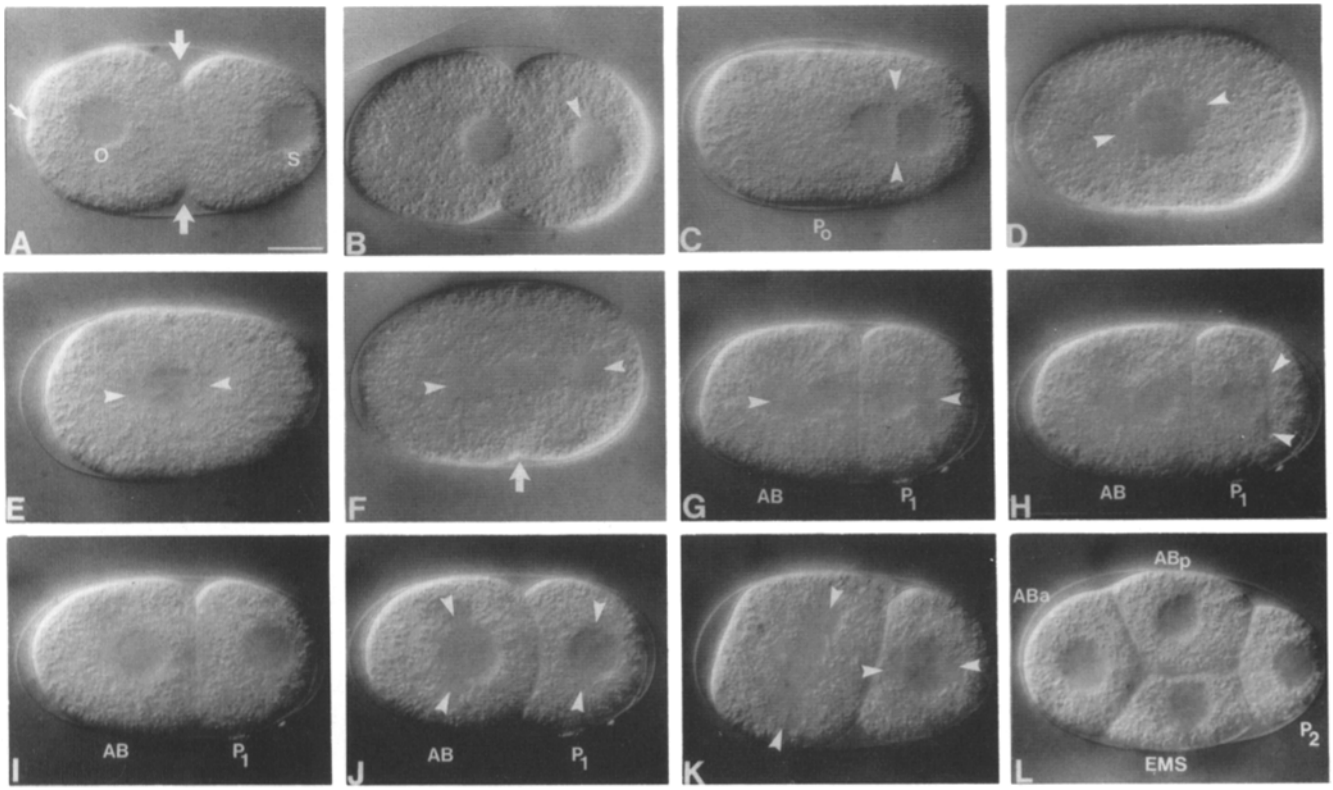

Figure 1. The first two cleavages in *Caenorhabditis elegans* embryogenesis (see Materials and Methods for details.) (*A*) PC furrow indicated by large arrows. *o*, oocyte pronucleus; *s*, sperm pronucleus. Cortical ruffling at anterior indicated by small arrow. (*B*) Arrowhead indicates one sperm centrosome; the other is out of focus. (*C*) Apposition of pronuclei results in the formation of the zygote, P_0. The sperm centrosomes are indicated by the arrowheads. The PC furrow has relaxed. (*D*) Arrowheads indicate sperm centrosomes after a rotation which aligns them along the anteroposterior axis (Hyman and White, 1987). (*E*) Nuclear membrane breakdown. (*F*) Large arrow indicates first manifestation of furrowing. Arrowheads mark poles of spindle, now asymmetrically placed. (*G*) Completion of first unequal cleavage producing the larger *AB* and smaller P_1. Arrowheads mark centrosomes. Note disc-shaped centrosome in P_1 displaced towards posterior and large centrally positioned centrosome in *AB*. (*H*) Centrosome splitting in P_1 is indicated by arrowheads. Note movement of P_1 nucleus away from the anterior cortex (compare with position of nucleus in *AB*). (*I*) Completion of posterior nuclear migration in P_1. (*J*) Centrosomes in *AB* and P_1 (*arrowheads*) are initially orthogonal to anteroposterior axis. (*K*) Centrosomes in P_1 (*arrowheads*) rotate so that they are aligned along the anteroposterior axis (Hyman and White, 1987). The spindle in *AB* begins to skew towards the anteroposterior axis during anaphase B (poles marked by *arrowheads*). (*L*) *AB* has cleaved equally to form *ABa* and *ABp*. P_1 has cleaved unequally to produce *EMS* (*larger*), and P_2 (*smaller*). Anterior to left; Bar, 10 μm.

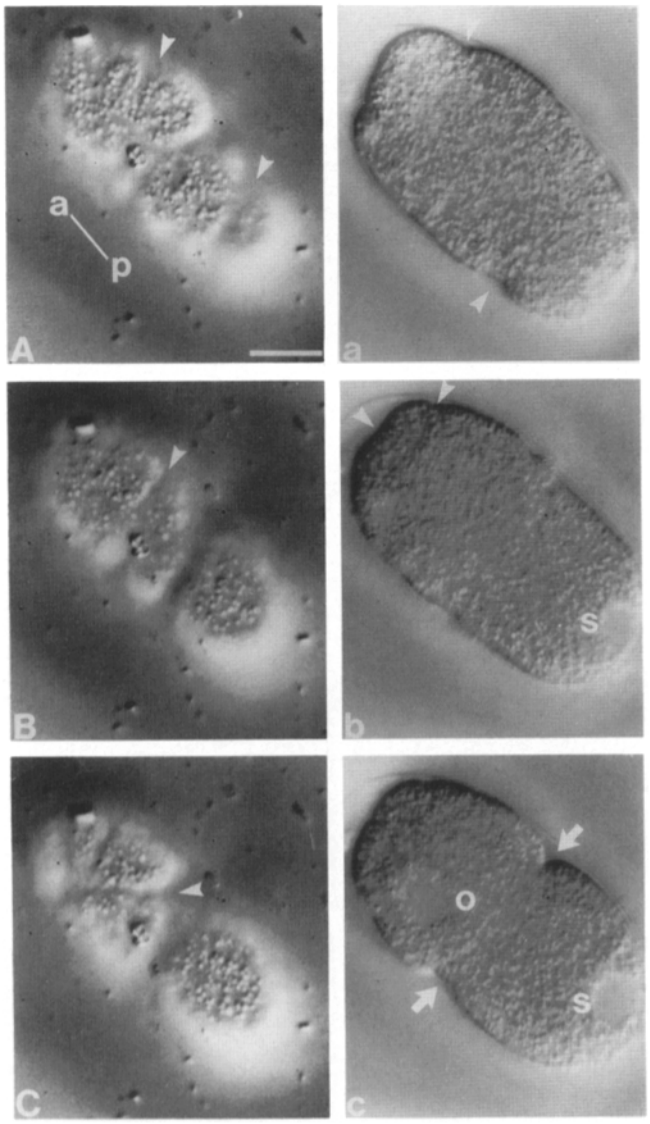

Figure 2. Cortical and cytoplasmic views of pseudocleavage. Anterior-posterior axis indicated. *A* and *a* show, respectively, a cortical and cytoplasmic plane view of an embryo early in PC using Nomarski optics. Ruffles seen on the surface of the embryo are marked with white arrowheads in both planes. They appear as "creases" on the surface and as constrictions at the sides of the embryo in the cytoplasmic plane. *B* and *b* show the cortical and corresponding cytoplasmic views, respectively, of the same embryo ~3 min after the preceding photographs. Note that the surface ruffling (*white arrowheads*) is now more restricted to the anterior half of the embryo. The sperm pronucleus (*s*) is indicated; the oocyte pronucleus is out of focus. *C* and *c* show that after an additional 3 min, the posterior surface is quiescent while the anterior surface continues to exhibit ruffling (*white arrowhead*). The PC furrow is now visible (*white arrows*) and the oocyte pronucleus (*o*) has begun to migrate towards the sperm pronucleus. Bar, 10 μm.

to the cell surface) during PC by means of a time lapse microscopy system that allows multiple focal levels to be recorded (see Materials and Methods). We tracked the position of individual cortical or cytoplasmic granules at successive time intervals and observed morphological changes on the cortex at the same time.

We found that early in PC (before the stage shown in Fig. 1 *A*) waves of cortical ruffling moved from the posterior end of the embryo towards the anterior where there was also vigorous cortical motile activity (Fig. 2 *A*, *a*). Later, the ruffling activity at the posterior end diminished (Fig. 2 *B*, *b*) although the anterior cortex continued to exhibit ruffling (Fig. 2, *B*, *b* and *C*, *c*). Granules adjacent to the plasma membrane in the posterior half of the embryo streamed from posterior to anterior towards the site where the PC furrow was starting to form (Fig. 3, *A* and *C*). This granule movement appeared as a flow of the entire field and was restricted to a layer of 2.5 μm thickness subjacent to the surface (corresponding to the cortex) in the posterior of the embryo. Cortical granules moved at speeds of 5.6 μm/min ± 1.3 (n = 46 granules, seven different embryos). Those in the anterior cortex did not exhibit such dramatic directed flow. They drifted slowly anteriorly, but with lateral excursions (Fig. 3, *A* and *C*).

At the same time as the cortical flow and anterior cortical motile activity, there was an oppositely oriented flow of granules in the cytoplasm. This posteriorly directed flow of cytoplasm was most apparent on the posterior side of the PC furrow (Fig. 3 *B*). As this flow was somewhat turbulent, it was difficult to quantitate, but by following large granules they could be seen to flow at ~4.4 ± 0.8 μm/min (n = 6 granules, 1 embryo). Granules in the cytoplasm anterior to the PC furrow did not exhibit this dramatic streaming, but did drift slowly posteriorly.

A continual reassociation of granules with the egg cortex at the posterior end of the egg must occur, as the posterior cortex did not become depleted of granules during the bulk cortical flow. Indeed, granules could be followed as they flowed through the cytoplasm to the posterior end, and then moved back towards the furrow in the opposite direction along the cortex (data not shown).

Both the cytoplasmic flow of the granules, and the flow of granules in the posterior cortex ceased around the time that the maternal pronucleus moved through the PC furrow to meet the paternal pronucleus (Fig. 1 *B*).

Differential Behavior of the Anterior and Posterior Cortices before, during, and after the First Cytokinesis

To gain a better understanding of the behavior of the cortex during true cytokinesis, we followed the movements made by the cell cortex throughout the first cleavage.

We found that during a period of ~2 min before the first morphological indication of furrowing, all of the granules on the posterior cortex up to the position where the furrow will form, repeatedly surged over distances of 2–3 μm in an anterior direction at speeds of up to 19 μm/min (Fig. 4 *A*). These rapid anterior movements were followed by slower posteriorly or laterally directed movements of <1 μm. In contrast, the granules on the anterior cortex moved in random directions and did not show these large displacements (Fig. 4 *A*).

Immediately after this asymmetric movement, the cytokinetic furrow became visible and deepened, and cortical granules began to flow into the furrow from both anterior and posterior sides. This second phase of cortical granule flow lasted for ~2 min with granules moving at 5.1 μm/min ± 1.1 (n = 10) during this time (Fig. 4 *B*).

A third phase of cortical granule flow then occurred im-

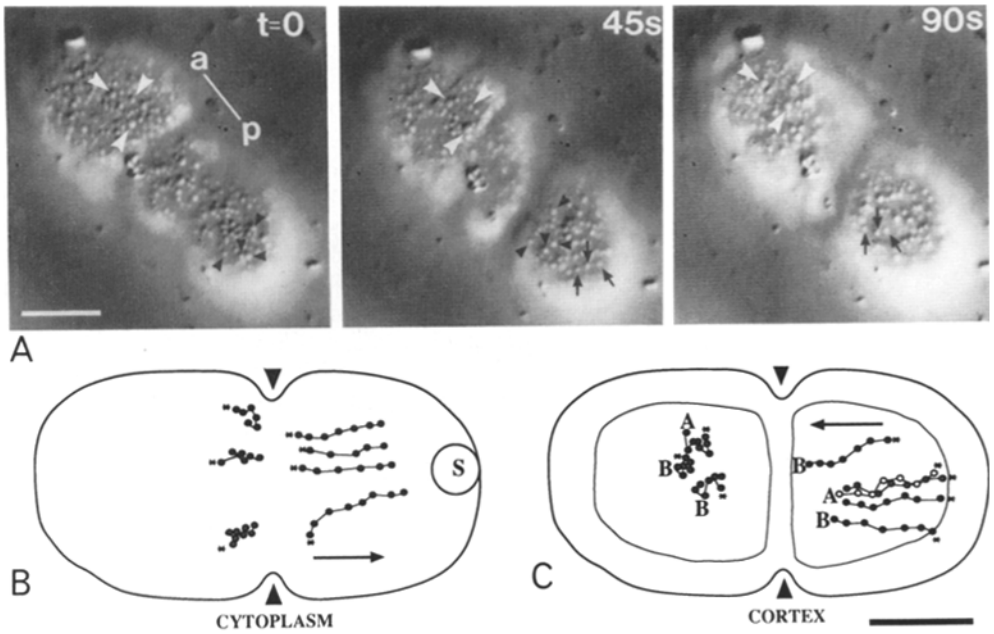

Figure 3. Cortical and cytoplasmic granule flow during PC at successive timepoints. Anteroposterior axis indicated. (*A*) The positions of cortical granules are marked with white arrowheads in the anterior and black arrows and arrowheads in the posterior. The time interval between successive images (from left to right) is 45 s. Identical arrows and arrowheads at different time points indicate the progress of the same set of granules. The granules in the posterior can be seen to move anteriorly, while those in the anterior move more randomly as they appear to drift slightly towards the anterior. Note how in the posterior, groups of granules retain the same approximate positions relative to each other as they flow anteriorly. The posterior granules chosen are representative of the entire field which is moving at this time. Bar, 10 μm. (*B*) The positions of cytoplasmic granules are plotted every 15 s in regions anterior and posterior to the PC furrow (*arrowheads*) in the same embryo. Asterisks mark the start of granule tracing. Note the posteriorly directed movement (*arrow*) of those granules posterior to the furrow. Anterior to left; Bar, 10 μm. (*C*) The positions of cortical granules are plotted every 15 s (*circles*) starting from two different time points *A* and *B* separated by 2 min. Asterisks mark the initial positions of granules. Granule positions shown are representative of the entire field. The position of the PC furrow is indicated by large black arrowheads. The contours of both the cortical (*inner*) and cytoplasmic (*outer*) views are shown for scale as they appear at the end of the migrations. Note the anteriorly directed movement of granules in the posterior (*arrow*). The paths of two granules in the posterior during time interval *A* can be seen to cross (*open* and *shaded circles*).

mediately after cytokinesis was completed, during the time in which the nucleus in P_1 migrated posteriorly through the cytoplasm (Fig. 1, *G–I*). At this time, all of the granules on the cortex of P_1 flowed anteriorly at 3.2 μm/min ± 1.1 (n = 33) with parallel, but not entirely straight, paths (Fig. 4 *C*). This movement in P_1 was continuous with the second phase. Meanwhile, the entire cortex of AB contracted vigorously and, apparently, randomly. However, unlike P_1, the granules on the cortex of AB moved randomly at this time with no net displacement (Fig. 4 *C*).

The migration of the P_1 nucleus occurred over a period of ~5 min with the nucleus moving at 1.9 μm/min ± 0.1 (n = 5). The fact that the P_1 nucleus migrated posteriorly during the time of P_1 anterior cortical flow suggests that the compensatory cytoplasmic flow might be driving the nucleus to the posterior. As the cytoplasmic flow during PC does not require intact microtubules (see below), we tested whether nocodazole would inhibit P_1 nuclear migration. In the presence of 10 μg/ml nocodazole P_1 nuclear migration was not prevented. Indeed, the nucleus migrated further than normal, until it was immediately adjacent to the posterior cortex (see Fig. 7 *A*). This is probably because the extensive astral microtubules normally impede such a close approach. We were unable to test for a requirement for actin microfilaments in nuclear migration because of the effect of cytochalasin D on cytokinesis: if the embryos were permeabilized to cytochalasin D at 1 μg/ml before the initiation of migration the cleavage furrow always regressed. Permeabilization without furrow regression could only be achieved after the nucleus had already moved some distance posteriorly.

Cortical Granule Flow during Pseudocleavage Does Not Depend on Microtubules, but Does Require Microfilaments

To determine whether microtubules play a role in the patterns of cortical flow that were observed during PC, we treated pronuclear stage embryos with the microtubule polymerization inhibitor nocodazole at 20 μg/ml (Fig. 5). At this concentration of nocodazole, astral microtubules are not visible, but very short microtubules are probably still present at the asters (Hyman and White, 1987). The PC furrow was often not as pronounced as in untreated embryos (Fig. 5 *C*). However, the cortical granule flow in the posterior appeared unaffected, with the field of granules moving at 3.5 ± 0.9 μm/min, (n = 16, 2 embryos). Cytoplasmic flow in the opposite direction also occurred at approximately the same rate as in untreated embryos (3.6 ± 0.6 μm/min, n = 18, 3 embryos). The cortical flow during PC does not depend therefore on the presence of microtubules, suggesting that the granules are not moving along microtubule tracks.

To see whether microfilaments are needed for the cortical movements of PC we treated pronuclear stage embryos with the microfilament inhibitor cytochalasin D at a concentration of 1 μg/ml. This concentration is sufficient to disrupt the cortical actin network (Strome, 1986) and block cleavage (Strome and Wood, 1983). Directed cortical granule flow was completely inhibited by cytochalasin D at 1 μg/ml (data not shown). Thus, the cortical movements seen during PC depend on the presence of intact microfilaments but not microtubules.

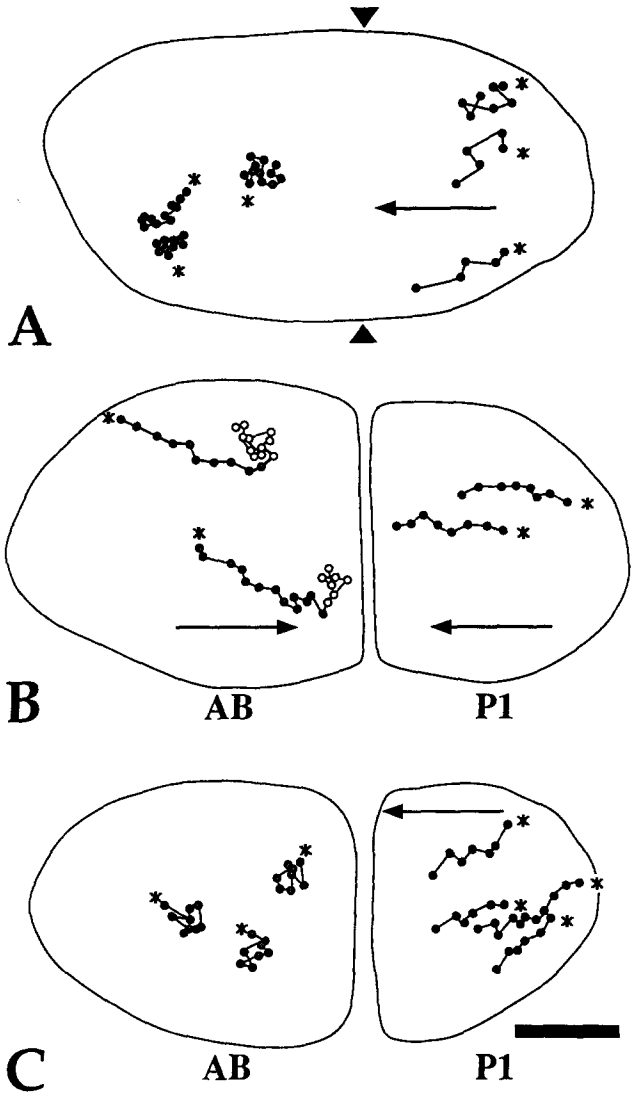

Figure 4. Cortical movements In *AB* and P_1 before, during, and after cytokinesis. Asterisks mark initial positions of granules. (*A*) Granule positions plotted every 9 s during a 1-min period before the cytokinetic furrow becomes visible. Arrowheads mark future position of cleavage furrow. Note difference in behavior between granules anterior to the future furrow (*shaded circles*) and those posterior (*black circles*). (*B*) Granule positions plotted every 9 s in same embryo as in (*A*) during period when cytokinetic furrow invaginates forming the anterior daughter cell *AB* and the posterior daughter cell P_1. In *AB*, the paths of two granules (*shaded circles*) are shown during this period when they exhibit anterior movement and then directly after (*open circles*) when they move randomly (as in *C*) at the completion of the cleavage furrow. Arrows indicate directions of granule movements. (*C*) Granule positions plotted every 15 s in a second embryo immediately after the completion of cytokinesis and during P_1 nuclear migration showing continued anterior migration of granules in P_1 and random movement in *AB*. Anterior to left. Bar, 5 μm.

Cortical and Cytoplasmic Granule Flow Is Observed during the Abortive Attempt at Cytokinesis after Microtubule Disruption

To determine whether the cortical granule flows seen during the first cytokinesis bear any similarities to those seen during PC, we followed the movement of cortical and cytoplasmic granules during the first cytokinesis in the presence of nocodazole at between 0.25 μg/ml–20 μg/ml (Fig. 5, *D–L*).

We examined the attempt at the first cleavage made by ~40 embryos treated with the drug from PC onwards. After PC in nocodazole-treated embryos, all manifestations of contractile activity and flow stopped at the same time as in untreated embryos, ~5 min before nuclear membrane breakdown (Fig. 5 *D*). If the embryo was treated with nocodazole after the migration of the sperm centrosomes to diametrically apposing positions on the sperm pronucleus, then a bipolar, attenuated spindle was formed (Strome and Wood, 1983; White and Hyman, 1987). This spindle had very short or no astral microtubules but did have short spindle microtubules (data not shown). It was positioned at the posterior end of the embryo as a result of the failure in pronuclear migration (Fig. 5, *F* and *H*). The attenuated spindle formed at the same time as it would in untreated embryos (~6 min after the end of the cortical activity), but was at right angles to the normal anterior-posterior spindle axis. Similar observations were made when previously untreated embryos were treated with nocodazole after the pronuclei had met.

At the time when an untreated embryo would be initiating cleavage, (~4 min after nuclear membrane breakdown), the nocodazole-treated embryo underwent a series of cortical and cytoplasmic movements. There was a flow of cytoplasm, at 5.8 ± 1.8 μm/min (n = 12 granules, 3 embryos) towards the posterior end (*large arrow*, Fig. 5 *F*). Simultaneously, all of the cortical granules flowed away from the posterior end (*arrow*, Fig. 5 *G*). The cortical granules moved at an average speed of 4.8 μm/min ± 0.9 (n = 31 granules, 10 embryos) in parallel paths throughout a depth of 2.5 μm from the cortex while the anterior cortex exhibited a vigorous series of contractions. These contractions were accompanied by the appearance of transient blebs which emanated from the anterior cortex (Fig. 5, *G–I*). A cleavage furrow (Fig. 5 *H*) invariably formed between the zone of directed cortical granule movement and the anterior zone of contraction. This furrow was distant from the attenuated spindle and was unusual in that, like the PC furrow, it did not bisect a mitotic spindle even though one was present in this case (White and Hyman, 1987). It also formed perpendicular to the axis bisecting the spindle (rather than along this axis as would normally happen). As in PC, the furrow did not go to completion; it regressed shortly after the nuclei reformed (Fig. 5 *K*).

An additional furrow was often initiated which did bisect the attenuated spindle and did go to completion (Fig. 5, *F* and *J*). The presence of this more conventionally orientated furrow was dependent on the length of the spindle, which in turn depended upon the concentration of inhibitor used. Spindles of length greater than 14 μm (obtained by using nocodazole concentrations of 0.25 μg/ml to 10 μg/ml) were capable of eliciting this bisecting furrow, while those around 14 μm often could not. Much smaller spindles (obtained through doses of inhibitor higher than 10 μg/ml) had poor morphology and were never seen to initiate the additional furrow.

Thus, nocodazole treatment essentially caused a replication of PC during first cleavage. Both normal PC and nocodazole-treated embryos at cytokinesis had oppositely oriented cortical and cytoplasmic flows, and nonspindle bisecting, regressive cleavage furrows.

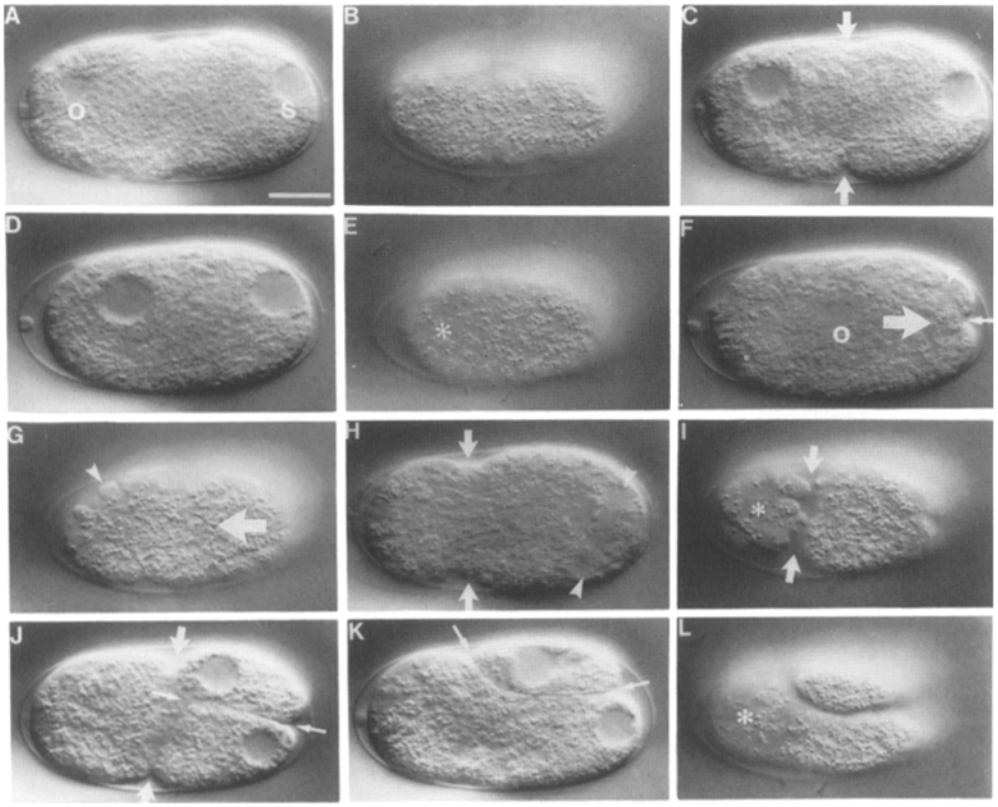

Figure 5. Effect of nocodazole on PC and the first cytokinesis. The drug was applied after the completion of the meiotic divisions and the sperm centrosome had been duplicated. (*A*) Embryo early in PC with contractions on both anterior and posterior surfaces. The pronuclei (*o*, oocyte; *s*, sperm) are visible at the poles of the embryo. (*B*) Top surface view of the same embryo at the same time as in *A*. Note how cortical granules are uniformly distributed on the anterior and posterior surfaces. (*C*) PC furrow (*arrows*) has now formed, but no pronuclear migration has occurred. (*D*) After PC, the furrow relaxes. The embryo then contracts at the anterior. The failure in pronuclear migration is evident. (*E*) Top surface view of *D*. Note how granules are now no longer uniformly distributed; the anterior surface (*asterisk*) has relatively few compared to the posterior surface. (*F*) An attenuated mitotic spindle has been set up around the sperm pronucleus and a furrow (*small arrow*) that bisects this spindle has been initiated. One pole of the spindle (*arrowhead*) is visible in this focal level. The direction of the cytoplasmic flow is indicated (*large arrow*). The membrane of the oocyte pronucleus (*o*) has broken down, and the nuclear contents are being swept along to the posterior by the cytoplasmic flow. (*G*) Top surface view at same time as *F*. Ruffling activity can be seen on the anterior surface (*arrowhead*) but not on the posterior. The direction of cortical flow is indicated (*arrow*). (*H*) The furrow bisecting the spindle that was initiated in *F* has regressed, presumably due to the force of the large flow of cytoplasmic material towards the posterior end of the embryo. Both poles of the spindle are now visible (*arrowheads*). A furrow has formed towards the anterior (*arrows*). The furrow does not bisect the attenuated spindle. (*I*) Top surface view of *H*. The cortex anterior to the furrow (*arrows* in *H*) exhibits dramatic and dynamic ruffling activity (*asterisk*) and is severely depleted of granules compared to the posterior cortex. This may be the result of the build up of actin in this region of the cortex (see Fig. 9) displacing and excluding the cortical granules. In many cases, fibrous structures with random orientation could be seen in these depleted areas (not shown). They appeared highly dynamic and had the same approximate dimensions as the actin bundles visualized by phallacidin staining of fixed embryos (<0.5 μm along their short axis). This raises the possibility that they are bundles of actin closely associated with the overlying membrane. (*J*) The spindle has been bisected by a furrow (*small arrows*) and two nuclei (containing the sperm chromosomes) have reformed. The anterior furrow is still visible (*large arrows*). Cleavage configuration aficionados may note the similarity to molluscan polar lobe formation (Conrad et al., 1973). (*K*) The anterior furrow has relaxed leaving two blastomeres. (*L*) Top surface view of *K* showing the depletion of granules from the region of the larger blastomere (*asterisk*) that was anterior to the regressive furrow. Anterior to left. Bar, 10 μm.

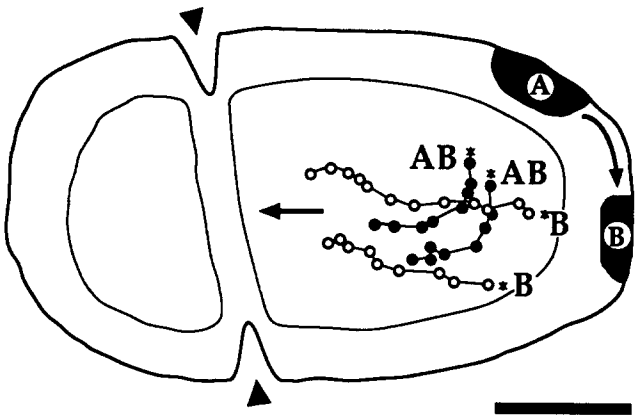

Figure 6. Cortical granule flow during attempt at cytokinesis in nocodazole-treated P_0. The initial and final positions of the attenuated spindle, *A* and *B*, are shown at the posterior. Granules that are moving as the attenuated spindle moves from *A* to *B* are colored black and labeled *AB*. Those that move after the remnant has reached position *B* are shown by open circles labeled *B*. In both cases, granule positions are plotted every 15 s. Granules which move as the attenuated spindle moves follow curved paths. The arrowheads mark the position of the transient, nonspindle bisecting furrow. Asterisks mark the initial positions of granules. Anterior to left. Bar, 10 μm.

The Position of the Attenuated Spindle in Nocodazole-treated Embryos Determines the Orientation of the Cortical and Cytoplasmic Flows during Attempted Cytokinesis

It was noticed that in three cases (out of 40) where a pronuclear stage embryo was treated with nocodazole, the attenuated spindle was eventually formed to one side of the anterior-posterior midline but still adjacent to the posterior cortex. When these embryos attempted to cleave, all of the

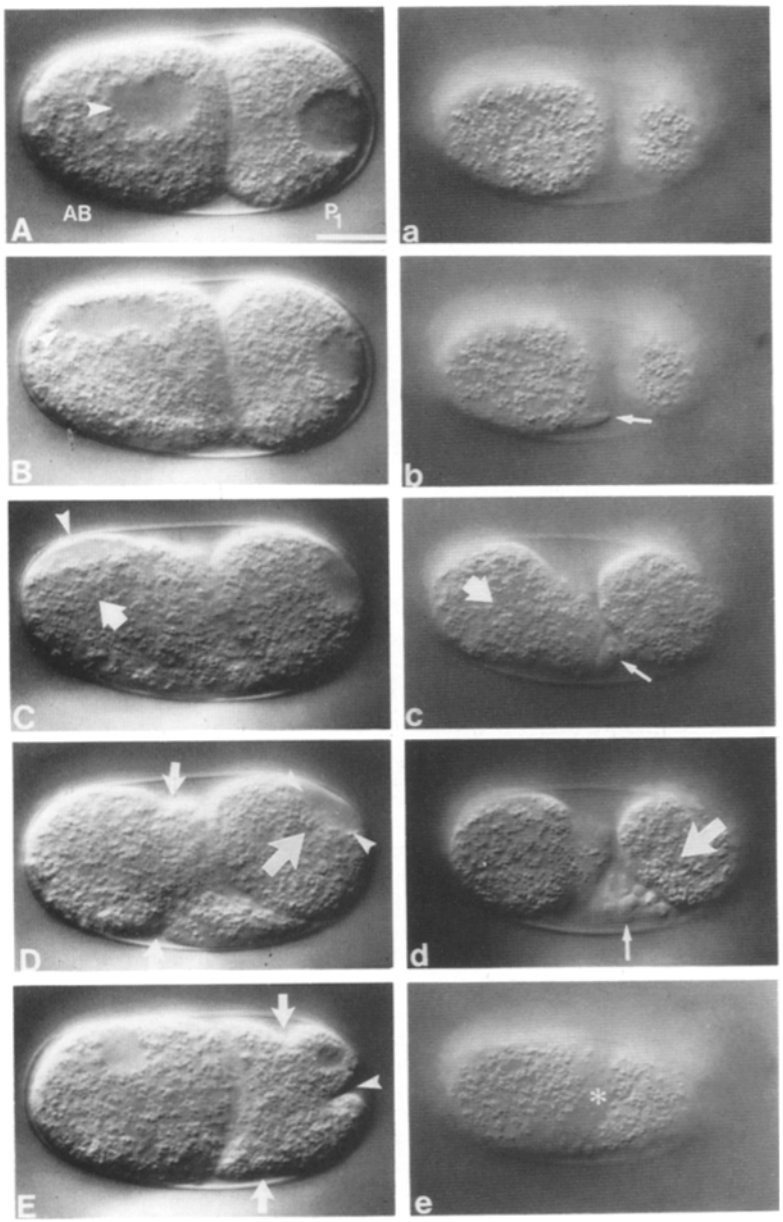

Figure 7. Effect of nocodazole on cleavage of *AB* and P_1. (*A*) Embryo permeabilized soon after first cleavage, before the *AB* centrosome has duplicated but after this event in P_1. Note how the P_1 nucleus has migrated to the extreme posterior. The nucleus and single centrosome (*arrowhead*) in *AB* are slightly displaced to one side of the embryo. (*a*) Cortical view of *A*. (*B*) A monopolar attenuated spindle has formed in *AB* adjacent to the cortex. The single aster is marked with an arrowhead. The nuclear membrane in P_1 is breaking down. (*b*) Top surface of *B* showing first manifestation of contractile activity in AB (*arrow*) opposite position of attenuated spindle. Such "blebs" are common in these regions. (*C*) Cytoplasmic flow (*arrow* indicates direction) in AB has extended cell. Position of attenuated spindle is shown (*arrowhead*). (*c*) Cortical view of *C* showing ruffles and depletion of granules on cortex opposite attenuated spindle (*small arrow*) similar to Fig. 5 *I*. The direction of the cortical flow is shown (*large arrow*). (*D*) Regressive cleavage furrow forms in AB (*arrows*) distant from MA. A bipolar, attenuated spindle is set up in P_1 (*arrowheads*) and the cortical and cytoplasmic flows are initiated. The spindle is invariably posterior because of the posterior placement of the centrosome at first cleavage and the further posterior migration of the nucleus and centrosomes after cleavage. The direction of cytoplasmic flow in P_1 is indicated (*large arrow*). (*d*) Dramatic blebbing seen in region of AB furthest from the attenuated spindle (*small arrow*). The direction of cortical flow in P_1 is indicated (*large arrow*). (*E*) Furrow has regressed in AB. Two furrows have formed in P_1; one bisects the MA (*arrowhead*), the other is parallel to and distant from the attenuated spindle (*arrows*). (*e*) Top surface view of *E* showing granule free region in AB (*asterisk*). Anterior to left. Bar, 10 μm.

cortical granules flowed away from the attenuated spindle, rather than away from the extreme posterior. The cytoplasmic flow was directed toward this region of the cortex, and often appeared to push the attenuated spindle around the cortex to the anterior-posterior midline. As the spindle moved, the direction of the cortical flow continually changed in concert so that the region of the cortex from which the granules moved was always overlying the attenuated spindle at that time. This had the consequence that cortical granules that were moving as the spindle traveled to the posterior followed curved paths as their direction changed (Fig. 6). To make sure that such curved trajectories were not the result of the embryo rolling about its long axis, we followed the movement of granules and blebs in the anterior portion. These remained relatively stationary.

Cortical granules that began their journey from the posterior after the attenuated spindle had moved followed essentially straight trajectories.

Cortical and Cytoplasmic Flows Are Seen in Nocodazole-treated Embryos at the Attempt at Second Cytokinesis

To see whether the cortical flows observed in drug treated embryos described above are unique to P_0 during its attempt at cytokinesis, we repeated the treatments in more than 40 two-cell embryos. After first cleavage, two-cell embryos were treated with 10 μg/ml nocodazole before the duplication of the AB centrosomes, but after this event in P_1. The nucleus in P_1 migrated to the posterior of the cell (Fig. 7 *A*) as in untreated embryos (see above). The nucleus in AB, by contrast, moved to a random position in the cell sometimes ending up close to the cortex.

AB then attempted to cleave at the same time as it would in untreated embryos ($\sim$3 min after nuclear membrane breakdown). A monopolar attenuated mitotic spindle was set up around the single centrosome. In many cases, the spindle

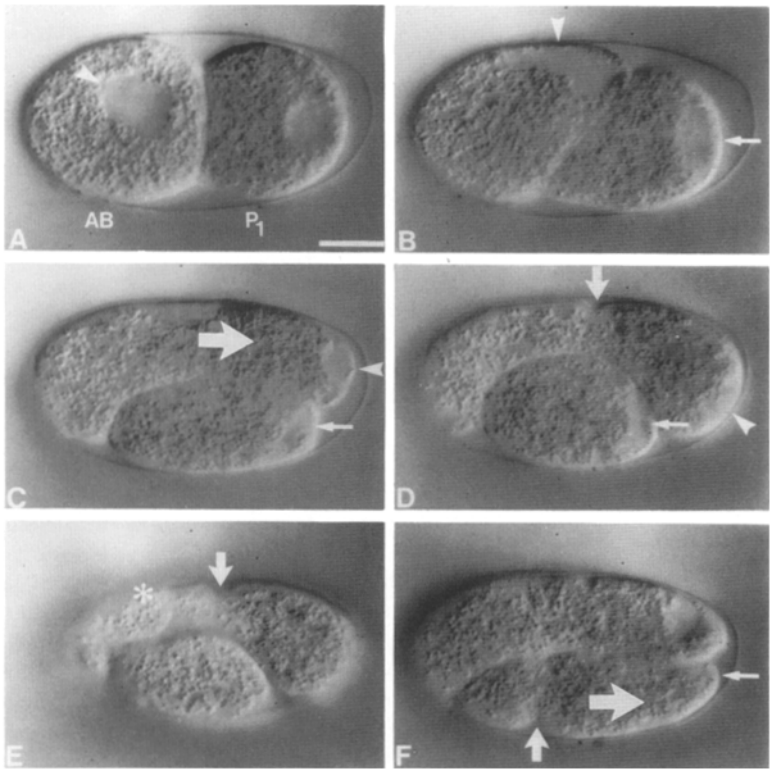

Figure 8. Extension of blastomeres at point adjacent to attenuated spindle during nocodazole-inhibited attempt at cytokinesis. (*A*) Embryo treated with 20 μg/ml nocodazole soon after first cleavage. The nucleus and centrosome in *AB* (*arrowhead*) are closest to a region of the cortex adjacent to P_1 that is not directly in contact with the eggshell. (*B*) A monopolar attenuated spindle (*arrowhead*) is formed in AB close to this region of the cortex. The P_1 nucleus breaks down at the posterior of the cell (*small arrow*). (*C*) AB becomes massively extended in a posterior direction as cortical and cytoplasmic flows are initiated during attempt at cleavage. The direction of the cytoplasmic flow is indicated (*large arrow*). The attenuated spindle invariably is at the leading edge of the extending cell in these cases (*arrowhead*). The attenuated spindle in P_1 is indicated by the small arrow. (*D*) AB is stretched over twice its normal anterior-posterior length. A transient furrow forms (*arrow*) which does not bisect the attenuated spindle. The spindle remnants in AB (*arrowhead*) and P_1 (*small arrow*) are indicated. Note how the posterior of P_1 now lies next to AB rather than next to the eggshell. (*E*) Top surface view of *d* showing ruffling (*asterisk*) anterior to the site of the regressive furrow in AB (*arrow*). (*F*) P_1 extends posteriorly during its attempt at cytokinesis. The direction of cytoplasmic flow is indicated (*large arrow*). The extension is possible because the posterior of P_1 is not in contact with the rigid eggshell after AB extension (see *D*). Note the formation of a furrow (*medium arrow*). Anterior to left. Bar, 10 μm.

was set up eccentrically, close to a random region of the cortex (Fig. 7 *B*). When the cortical flow commenced in these situations it moved granules away from the area of the cortex nearest to the attenuated spindle, again with the cytoplasmic flow directed towards it (Fig. 7 *C* and *c*). It was therefore possible to predict the direction of the cortical and cytoplasmic flows if the attenuated spindle was initially eccentrically positioned. As the attenuated spindle was eccentrically placed before the flows began, this observation is further evidence that the position of the attenuated spindle is the determinant of the subsequent flow directions. The cortex distal from the attenuated spindle underwent a series of contractions and blebbing (Fig. 7, *b–d*) similar to the anterior cortex in drug-treated embryos at first cleavage, and a transient cleavage furrow was formed which did not bisect the attenuated spindle (Fig. 7 *D*).

In cases where the monopolar spindle in AB was formed in the middle of the cell, the cortical flow was initiated in a random direction with the concomitant cytoplasmic flow in the reverse direction. The attenuated spindle moved towards the cortex in the direction of the cytoplasmic flow, and was probably carried by it.

P_1 attempted to cleave at the same time as it would normally, ~2 min after AB. In contrast to the apparently random location of the attenuated spindle in AB, the attenuated bipolar spindle in P_1 was always set up at the posterior end of the cell (Fig. 7 *D*). The cortical flow was invariably in the posterior to anterior direction, and the cytoplasmic flow was in the reverse direction (*large arrows* in Fig. 7, *D* and *d*). A regressive furrow was formed parallel to the bipolar spindle (Fig. 7 *E*, *arrows*). Depending on the concentration of nocodazole, and hence the length of the spindle, an additional furrow was formed which did bisect the P_1 spindle (Fig. 7 *E*, *arrowhead*).

In a small number of embryos examined (five), the attenuated spindle in AB was seen to form close to a cortical domain which was not directly bounded by the chitinous eggshell (Fig. 8, *A–B*). In these situations, AB became massively extended in this region during the attempt at cytokinesis, filling the void volume (Fig. 8, *B–D*).

Cortical Actin Distribution in Cells Undergoing Nocodazole-inhibited Cytokinesis

To see how the cortical actin network is organized during nocodazole-inhibited cytokinesis, treated cells were fixed and stained with Bodipy-phallacidin to visualize filamentous actin. Approximately 100 embryos were examined. It was often difficult to obtain a coherent picture of the actin distribution during the attempt at cytokinesis because of the highly irregular contour of the cell cortex. This was probably the result of the extensive ruffling activity observed in areas of the cortex distant from the attenuated spindle. Filamentous actin appeared to be located predominantly in the cortex (Fig. 9 *A*).

In cells which were in the early stages of the attempt at cytokinesis, the cortex was less distorted and therefore easier to examine. The region of the cortex distant from the attenuated spindle often stained more heavily than regions closer to the attenuated spindle. This was especially obvious in the

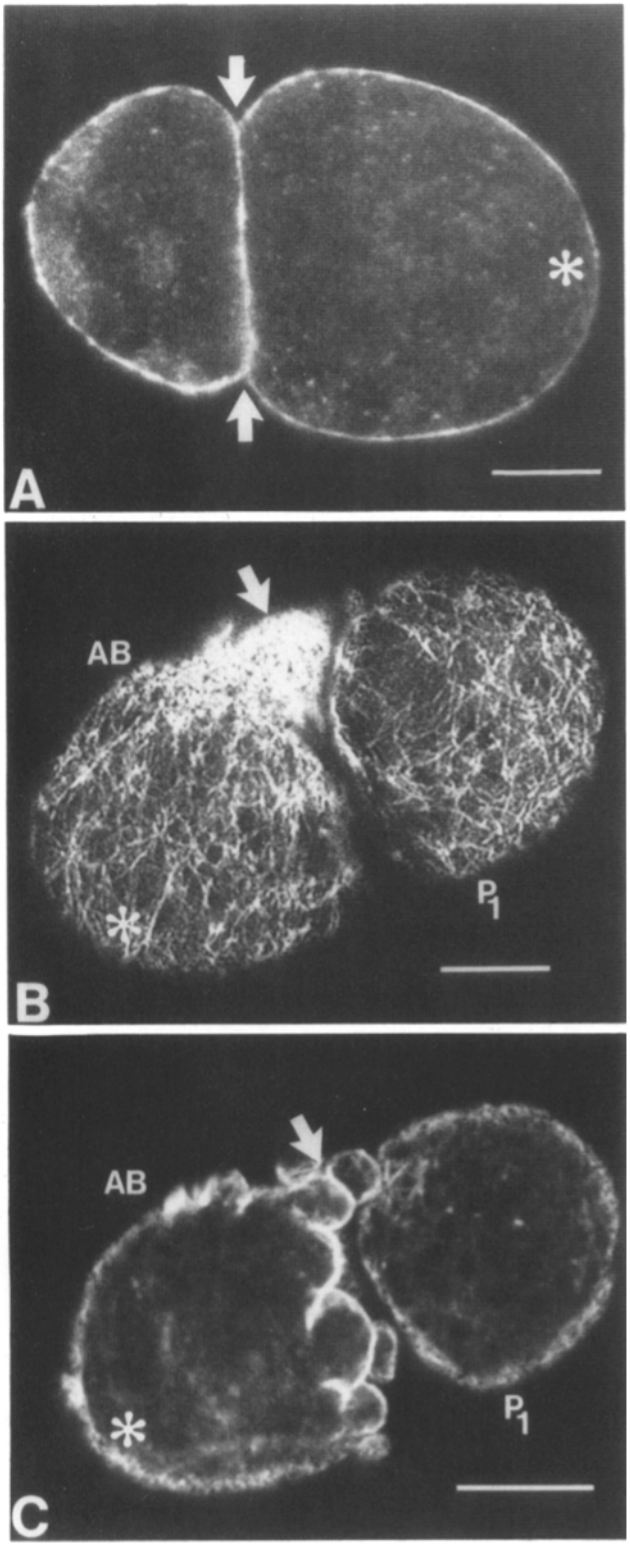

Figure 9. Fluorescent phallacidin staining of filamentous actin in embryos treated with nocodazole before cytokinesis. (*A*) One cell embryo after first attempt at cytokinesis viewed in a cytoplasmic plane. Asterisk shows position of chromosomes on attenuated spindle. Arrows indicate the transient furrow. Note the predominantly cortical localization of actin. (*B*) Beginning of attempt at cytokinesis in nocodazole-treated *AB* cell viewed in the plane of the cortex. Arrow shows actin build up in the initial protrusion which forms distant from the attenuated spindle (*asterisk*). (*C*) Blebbing (*arrowhead*) on the surface of another *AB* cell during attempt at cytokinesis (similar to that seen in Fig. 7 *d*) viewed just below the cortical plane. The blebbing activity is restricted to the region of the cortex opposite the attenuated spindle (*asterisk*). Cortical actin is more abundant in the vicinity of the blebs than elsewhere in the cortex. Anterior to left. Bar, 10 μm.

protrusions and blebs that formed distant from the attenuated spindle. The increased staining could be seen in cortical views as an increase in fiber density (Fig. 9 *B*, *arrow*) and in cytoplasmic views as brighter cell periphery staining. The cortical blebs which appear later in the attempt at cytokinesis (such as in Fig. 7 *d*) are ringed with actin (Fig. 9 *C*, *arrow*). These also appear to stain more heavily for actin than other regions of the cortex.

Discussion

The Flow Patterns of PC and Nocodazole-inhibited Cytokinesis Are Determined by the Position of the Centrosomes

We have described the patterns of cortical and cytoplasmic flow during PC, during an asymmetric division, and during nocodazole-inhibited cytokinesis in *C. elegans* blastomeres. During PC, cytoplasm flows from the anterior to the posterior end of the fertilized oocyte (Nigon, 1960). This cytoplasmic flow is accompanied by a cortical flow of granules in the reverse (posterior to anterior) direction and the formation of a transient cytokinetic furrow. This flow pattern requires actin microfilaments, but not long microtubules. There is evidence that the cytoplasmic flow carries determinants and other factors (such as P granules) to the posterior end of the egg so that they are inherited by the posterior daughter, P_1, at first cleavage (for review see Strome, 1989). These segregative events are required for the determinative nature of the division. How is the polarity of the flows specified?

The cleavage configuration of blastomeres treated with the microtubule polymerization inhibitor nocodazole before cytokinesis is very similar to PC. Moreover, cytoplasmic and cortical flows are seen during both PC and nocodazole-inhibited cytokinesis. The direction of these flows in nocodazole-treated cells is specified by the position of the attenuated mitotic apparatus. Can the similarities between nocodazole-inhibited cytokinesis and PC reveal how the polarity of the PC flow is specified? Although there is no mitotic apparatus (MA) present during PC, sperm asters (centrosomes and associated microtubules) are present at the posterior end of the egg (Hyman and White, 1987). It is therefore possible that the sperm asters induce and orient the cortical and cytoplasmic flows and the transient furrow in the same way as the attenuated MA does in nocodazole-treated cells. If these flows are responsible for the expression of anterior-posterior polarity in the egg, then the position of the sperm centrosome at fertilization could determine the anteroposterior axis.

Behavior of the Cortex during an Asymmetric Division

The first cell division in *C. elegans* is unequal because of the posterior movement of the MA during anaphase (Albertson,

1984). After the furrow is completed, cortical material flows from posterior to anterior in P_1, but not in AB. AB normally divides proliferatively, giving rise to daughters of equivalent developmental potential (Priess and Thomson, 1987). At the same time as the cortical flow in P_1, its nucleus and associated centrosomes migrate posteriorly through the cytoplasm. This movement does not require microtubules, but may require microfilaments. It is likely that the nucleus is driven posteriorly by the flow of cytoplasm necessary to balance the cortical flow in the opposite direction. Thus, there is a polarized flow of cytoplasm and cortex in P_1 which subsequently divides unequally to give daughters with distinct fates, but no flow in AB which divides equally. P_1 segregates P granules to the posterior at about the same time as the flow occurs (Strome and Wood, 1982). P granules, and other cytoplasmic factors necessary for the determinative nature of the subsequent cleavage, could be swept to the posterior by the cytoplasmic component of the flows. Conversely, factors associated with the cortex in P_1 would be segregated to the anterior of the cell. In both cases, specific "tethers" for the factors would be required to keep them localized. Cytoplasmic localization would not be expected to occur in AB, so no flow would be required.

Polarized flows of cytoplasmic and cortical material were observed in nocodazole-treated P_0, P_1, and AB cells. Both P_0 and P_1 normally undergo unequal, determinative divisions, and so have some intrinsic polarity. AB would not be expected to have any polarized characteristics, yet under the conditions described it behaves in a polarized manner. This indicates that the ability to generate the directed flows of material is not unique to polarized cells, but can occur in other cleaving cells with eccentrically located aster(s). It will be intriguing to see if the direction of cytoplasmic and cortical movements in other embryonic blastomeres can be similarly correlated with the position of microtubule organizing centers.

The Flow Patterns May be Due to Movement of the Actin Cytoskeleton

Cytokinesis results from the formation of the contractile ring comprised of circumferentially oriented actin microfilaments, myosin, and a host of accessory proteins (for review see Mabuchi, 1986; Salmon, 1989; Satterwhite and Pollard, 1992). The actin component of the contractile ring is probably formed from preexisting cortical actin microfilaments, which flow from the poles of the cell towards the equatorial region along the cortex (Cao and Wang, 1990*a*,*b*). Membrane receptors (McCaig and Robinson, 1982; Koppel et al., 1982), and cortical organelles (Dan, 1954) have been seen to flow towards the equatorial region during cytokinesis, and may be driven there by the cortical actin movements (Holifield et al., 1990). The cortical flows observed in *C. elegans* were inhibited by cytochalasin D treatment implying that they required filamentous actin. As the flows occurred at the time that an untreated cell would be initiating cytokinesis, it is possible that they result from the movements of cortical actin that would normally generate a contractile ring. These actin movements have become redirected because of the unusual size and/or location of the MA. During both PC and nocodazole inhibited cytokinesis, the cytoplasmic flow would compensate for the movement of the cortical material.

Actin based cortical flows have been documented in several motile systems (Wang, 1985; Forscher and Smith, 1988; Okabe and Hirokawa, 1991; Theriot and Mitchison, 1991) and involve the polymerization of actin at the leading edge of the cell (Okabe and Hirokawa, 1989; Symons and Mitchison, 1991) followed by the movement of filaments away from the leading edge. The flow of material on the surface of such cells can be attributed to their interactions with the moving actin network in some, but not all, cases (Forscher and Smith, 1990; Theriot and Mitchison, 1992). The flows that we have described occur at rates consistent with the hypothesis that they are being driven by cortical actin flow. The force responsible for the actin movement is probably actomyosin based, but may also be driven by localized actin polymerization (for review see Bray and White, 1988; Mitchison and Kirschner, 1988; Smith, 1989).

The direction of the cortical flow during PC and nocodazole-inhibited cytokinesis is correlated with the position of the attenuated aster(s). This suggests that some component of the asters induces the movement of the cortical actin network away from the area in which they are located. This may explain why a redistribution of cortical actin is seen during PC (Strome, 1986) and nocodazole-inhibited cytokinesis (Fig. 9). The compensating cytoplasmic flow back towards the aster(s) could return monomeric actin for polymerization into the network so that the cortical flow would be maintained (Bray and White, 1988). The monomeric actin could be supplied by the contractile ring which disperses actin as it tightens (Schroeder, 1972). The component of the asters that is responsible for the induction of the flows could either be the centrosomes or the astral microtubules (very short microtubule "stubs" are probably still present at the centrosomes in nocodazole-treated blastomeres).

Interaction between the Centrosomes and Cortex during Cytokinesis

We have suggested that the polarized flows of cortical material seen during PC and nocodazole-inhibited cytokinesis result from the induction of a directed cortical flow by eccentrically located aster(s). In the case of nocodazole-treated cells, how does this relate to the normal action of the MA during cytokinesis? At least in large embryonic cells, the asters of the MA determine the position of the contractile ring such that the furrow always forms between them (for review see Rappaport, 1986). Just before furrowing, the cortex of a cell is in a state of uniform tension, but as cytokinesis is initiated, tension falls off at the poles and increases at the equator (Hiramoto, 1987). This gradient of cortical tension is initiated by the asters (Rappaport, 1986), and would result in the movement of the actin network (and associated cortical material) away from the lower tension polar regions towards the higher tension equatorial region where filaments align circumferentially to form the contractile ring (White and Borisy, 1983). The asters could create this tension gradient by one or a combination of two mechanisms: (*a*) stimulation of cortical tension at the equator (Rappaport, 1986; Devore et al., 1989); and (*b*) relaxation of cortical tension away from the equator (Wolpert, 1960; Schroeder, 1981; White and Borisy, 1983). Both result in the same final tension differential (Fig. 10, *A–C*). If the asters relax the cortical tension in their vicinity, then displacing them both to one region of the

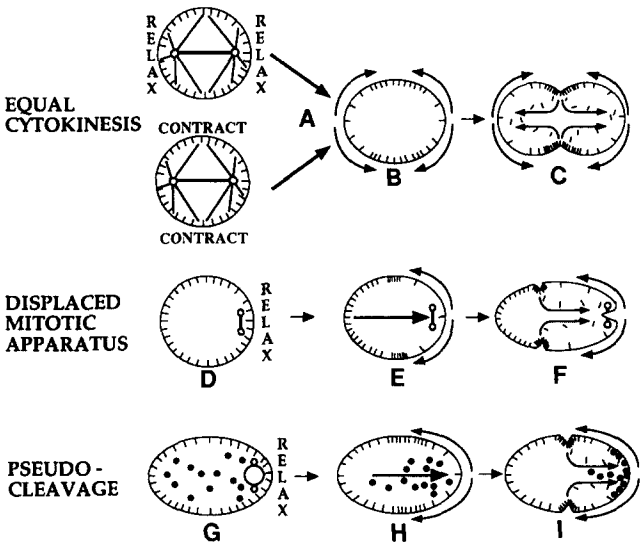

Figure 10. Schematic diagram of cortical movements during an equal cytokinesis, cytokinesis with a displaced MA and PC. In each figure, the density of actin/myosin contractile elements is represented by radially distributed lines. Internal arrows represent cytoplasmic movements; external arrows depict cortical movements. (*A–C*) Equal cytokinesis. Cytokinesis is initiated by one or both of Relaxation (*RELAX*) of cortical tension at the poles/Contraction (*CONTRACT*) of the equatorial cortex. Both result in the movement of cortical material away from the poles to the equatorial region (*curved arrows* in *B*). The contractile elements assemble into the contractile ring which disperses actin as it tightens (*C*). The dispersed actin may be carried back to the poles through the cytoplasm (*curved internal arrows* in *C*). (*D–E*) Displaced mitotic apparatus (as would occur during nocodazole treatment). The MA forms close to the cortex (*D*). If the poles of the MA relax the cortical tension at this point (*D*), then cortical material would flow away from it (*curved arrows* in *E*). Cytoplasm would flow towards the MA (*straight arrow* in *E*). The cortical tension elements migrate rapidly away from the aster, slow down distant from it, and pile up in a wavefront that can contract and form a contractile ring which does not bisect the mitotic apparatus (*F*). An additional spindle bisecting furrow would form if the poles of the MA are sufficiently far apart. The cytoplasmic flow could carry actin from the dispersing contractile ring back towards the MA (*curved internal arrows* in *F*). (*G–I*) Model for pseudocleavage. Anterior is at the left. Some component of the asters of the sperm pronucleus induces relaxation of cortical tension at the posterior end of the egg (*G*). This induces a movement of contractile elements from this end (*curved arrows* in *H*), and a simultaneous flow of cytoplasm towards this (*straight arrow* in *H*). A contractile ring which gives rise to the PC furrow (*I*) forms as described above. P granules (*black circles*) may be segregated to the posterior end of the egg by the cytoplasmic flow. Actin may also be carried through the cytoplasm for repolymerization at the posterior (see *D–I*).

cortex would be expected to cause the actin network to be pulled away from that area and cytoplasm towards it. Conversely, if they normally stimulate cortical tension then the opposite flow patterns would be predicted, as the cortical region next to the MA would be activated and would therefore contract. The flow patterns that are seen when the MA is displaced with nocodazole are more consistent with the relaxation model (Fig. 10, *D–F*). Nocodazole-treated cells are capable of dramatic extension at the region of the cell next to the eccentric MA, suggesting that the cortex is indeed relatively relaxed there (Fig. 8). This relaxation would be initiated in the nocodazole-treated cells by either the centrosomes or the remaining very short astral microtubules. PC may also be initiated by the sperm centrosomes or asters acting to relax cortical tension at the posterior of the egg (Fig. 10, *G–I*).

The Transient Furrow Seen during PC and Nocodazole-inhibited Cytokinesis May Result from the Relaxation of Cortical Tension by the Asters

The actin network may move in response to differences in cortical tension, such that it always moves up a tension gradient. This could explain why it moves towards the equator during cytokinesis. Computer simulations of the cortex in an elongated cell in which the mitotic asters are close to the cortex predict the appearance of two furrows, one from each aster, if the asters act to relax the tension (White and Borisy, 1983). These furrows form because of rapid migration of the actin network away from the vicinity of each aster. The network slows down at some distance from the aster and piles up in a wavefront which can contract to generate a contractile ring. The transient furrows that are seen during PC and nocodazole-inhibited cytokinesis may form in this way (White and Hyman, 1987). An additional "conventional" furrow that does bisect the MA was sometimes observed in nocodazole-treated cells. The fact that this furrow, unlike the non-bisecting cases, can go to completion suggests that some component of the spindle itself is required to complete the furrow. The presence of the bisecting furrow depends on the length of the bipolar MA, with centrosomes <14 μm apart being unable to elicit it. Sperm asters are ~10 μm apart during PC, perhaps explaining why a furrow that bisects the sperm pronucleus/aster complex does not form during PC.

We thank Viki Allan, Julie Ahringer, Mark Bretscher, Bob Goldstein, John Kilmartin, Benjamin Podbilewicz, and Susan Strome for critical comments on the manuscript. We also thank Susan Strome for communicating unpublished results.

Received for publication 16 February 1993 and in revised form 31 March 1993.

References

Abercrombie, M., J. E. M. Heaysman, and S. M. Pegrum. 1970. The locomotion of fibroblasts in culture. III. Movements of particles on the dorsal surface of the leading lamellae. *Exp. Cell Res.* 62:389–398.

Albertson, D. G. 1984. Formation of the first cleavage spindle in nematode embryos. *Dev. Biol.* 101:61–72.

Bray, D., and J. G. White. 1988. Cortical flow in animal cells. *Science (Wash. DC).* 239:883–888.

Brenner, S. 1974. The genetics of *Caenorhabditis elegans*. *Genetics.* 77: 71–94.

Bretscher, M. S. 1976. Directed lipid flow in cell membranes. *Nature (Lond.).* 260:21–23.

Bretscher, M.S. 1984. Endocytosis: relation to capping and cell locomotion. *Science (Wash. DC).* 224:681–686.

Cao, L.-G., and Y-L. Wang. 1990*a*. Mechanism of formation of contractile ring in dividing cultured animal cells. I. Recruitment of preexisiting actin filaments into the cleavage furrow. *J. Cell Biol.* 110:1089–1095.

Cao, L.-G., and Y-L. Wang. 1990*b*. Mechanism of formation of contractile ring in dividing cultured animal cells. II. Cortical movement of microinjected actin filaments. *J. Cell Biol.* 111:1905–1911.

Conrad, G. W., D. C. Williams, F. R. Turner, K. M. Newrock, and R. A. Raff. 1973. Microfilaments in the polar lobe constriction of fertilized eggs of *Ilynassa obselata*. *J. Cell Biol.* 59:228–233.

Dan, K. 1954. The cortical movement in *Arbacia punctulata* eggs through cleavage cycles. *Embryologia.* 2:115–122.

Devore, J. J., G. W. Conrad, and R. Rappaport. 1989. A model for astral stimu-

lation of cytokinesis in animal cells. *J. Cell Biol.* 109:2225–2232.
Edgar, L. G., and J. D. McGhee. 1986. Embryonic expression of a gut specific esterase in *Caenorhabditis elegans*. *Dev. Biol.* 114:109–118.
Fisher, G. W., P. A. Conrad, R. L. DeBiasio, and D. L. Taylor. 1988. Centripetal transport of cytoplasm, actin and the cell surface in lamellipodia of fibroblasts. *Cell Motil. Cytoskeleton.* 11:235–247.
Forscher, P., and S. J. Smith. 1988. Action of cytochalasins on the organization of actin filaments and microtubules in a neuronal growth cone. *J. Cell Biol.* 107:1505–1516.
Forscher, P., and S. J. Smith. 1990. Cytoplasmic actin filaments move particles on the surface of the nerve growth cone. *In* Optical Microscopy for Biology. B. Herman and K. Jacobson, editors. Wiley-Liss, New York. 459–471.
Grebecki, A. 1984. Relative motion in *Amoeba proteus* in respect to the adhesion sites. I. Behavior of montactic forms and the mechanism of fountain phenomenon. *Protoplasma.* 123:116–134.
Heath, J. P. 1983. Behaviour and structure of the leading lamella in moving fibroblasts. I. Occurrence and centripetal movement of arc-shaped microfilament bundles beneath the dorsal cell surface. *J. Cell Sci.* 60:331–354.
Hill, D. P., and S. Strome. 1988. An analysis of the role of microfilaments in the establishment and maintenance of assymetry in *Caenorhabditis elegans* zygotes. *Dev. Biol.* 125:75–84.
Hill, D. P., and S. Strome. 1990. Brief cytochalasin-induced disruption of microfilaments during a critical interval in 1 cell *C. elegans* embryos alters the partitioning of developmental instructions to the 2 cell embryo. *Development.* 108:159–172.
Hiramoto, Y. 1987. Mechanical properties of the protoplasm of echinoderm eggs at various stages of cell cycle. *In* Biomechanics of Cell Division. NATO ASI Series. N. Akkas, editor. Plenum, New York. 13–32.
Hirsh, D., D. Oppenheim, and M. Klass. 1976. Development of the reproductive system of *Caenorhabditis elegans* . *Dev. Biol.* 49:200–219.
Holifield, B. F., and K. Jacobson. 1991. Mapping trajectories of Pgp-1 membrane protein patches on surfaces of motile fibroblasts reveals a distinct boundary separating capping on the lamella and forward transport on the retracting tail. *J. Cell Biol.* 98:191–203.
Holifield, B. F., A. Ishihara, and K. Jacobson. 1990. Comparative behavior of membrane protein–antibody complexes on motile fibroblasts: implications for a mechanism for capping. *J. Cell Biol.* 111:2499–2512.
Hyman, A. A., and J. G. White. 1987. Determination of cell division axes in the early embryogenesis of *Caenorhabditis elegans*. *J. Cell Biol.* 105: 2123–2135.
Kirby, C., M. Kusch, and K. Kemphues. 1990. Mutations in the *par* genes of *Caenorhabditis elegans* affect cytoplasmic reorganization during the first cell cycle. *Dev. Biol.* 142:203–215.
Koppel, D. E., J. M. Oliver, and R. D. Berlin. 1982. Surface functions during mitosis. III. Quantitative analysis of ligand-receptor movement into the cleavage furrow: diffusion vs. flow. *J. Cell Biol.* 93:950–960.
Kucik, D. F., E. L. Elson, and M. P. Sheetz. 1990. Cell migration does not produce lipid flow. *J. Cell Biol.* 111:1617–1622.
Lee, J., M. Gustafsson, K.-E. Magnusson, and K. Jacobson. 1990. The direction of lipid flow in locomoting polymorphonuclear leukocytes. *Science (Wash. DC).* 247:1229–1233.
McCaig, C. D., and K. R. Robinson. 1982. The distribution of lectin receptors on the plasma membrane of fertilized sea urchin egg during first and second cleavage. *Dev. Biol.* 92:197–202.
Mabuchi, I. 1986. Biochemical aspects of cytokinesis. *Int. Rev. Cytol.* 101: 175–213.
Mitchison, T. J., and M. Kirschner. 1988. Cytoskeletal dynamics and nerve growth. *Neuron.* 1:761–772.
Nigon, V., P. Guerrier, and H. Monin. 1960. L'architecture polaire de l'oeuf et les movements des constituants cellulaires au cours des premieres etapes du developpement chez quelques nematodes. *Bull. Biol. Fr. Belg.* 94:131–202.
Okabe, S., and N. Hirokawa. 1989. Incorporation and turnover of biotin labeled actin microinjected into fibroblastic cells: an immunoelectron microscopic study. *J. Cell Biol.* 109:1581–1595.
Okabe, S., and N. Hirokawa. 1991. Actin dynamics in growth cones. *J. Neurosci.* 11:1918–1929.
Priess, J. R., and J. N. Thomson. 1987. Cellular interactions in early *C. elegans* embryos. *Cell.* 48:241–250.
Rappaport, R. 1986. Establishment of the mechanism of cytokinesis in animal cells. *Int. Rev. Cytol.* 101:245–281.
Salmon, E. D. 1989. Cytokinesis in animal cells. *Curr. Opin. Cell Biol.* 1:541–547.
Satterwhite, L. L., and T. D. Pollard. 1992. Cytokinesis. *Curr. Opin. Cell Biol.* 4:43–52.
Schroeder, T. E. 1972. The contractile ring. II. Determining its brief existence, volumetric changes and vital role in cleaving *Arbacia* eggs. *J. Cell Biol.* 53:419–434.
Schroeder, T. E. 1981. The origin of cleavage forces in dividing eggs. *Exp. Cell Res.* 134:231–240.
Sheetz, M. P., S. Turney, H. Quian, and E. L. Elson. 1989. Nanometre-level analysis demonstrates that lipid flow does not drive membrane glycoprotein movements. *Nature (Lond.).* 340:284–288.
Smith, S. J. 1988. Neuronal cytomechanics: the actin based motility of growth cones. *Science (Wash. DC.)* 242:708–715.
Strome, S. 1986. Fluorescence visualization of the distribution of microfilaments in gonads and early embryos of *Caenorhabditis elegans*. *Dev. Biol.* 107:337–354.
Strome, S. 1989. Generation of cell diversity during early embryogenesis in the nematode *Caenorhabditis elegans*. *Int. Rev. Cytol.* 114:81–123.
Strome, S., and W. B. Wood. 1982. Immunofluorescence visualization of germ-line-specific cytoplasmic granules in embryos, larvae, and adults of *Caenorhabditis elegans*. *Proc. Natl. Acad. Sci. USA.* 79:1558–1562.
Strome, S., and W. B. Wood. 1983. Generation of asymmetry and segregation of germ-line granules in early *C. elegans* embryos. *Cell.* 35:15–25.
Sulston, J. E., E. Schierenberg, J. G. White, and J. N. Thomson. 1983. The embryonic cell lineage of the nematode *Caenorhabditis elegans*. *Dev. Biol.* 100:64–119.
Symons, M. H., and T. J. Mitchison. 1991. Control of actin polymerization in live and permeabilized fibroblasts. *J. Cell Biol.* 114:503–513.
Taylor, R. B., W. Duffus, H. Philip, M. C. Raff, and S. De Petris. 1971. Redistribution and pinocytosis of lymphocyte surface immunoglobulin molecules induced by anti-immunoglobulin antibodies. *Nat. New Biol.* 233:225–229.
Theriot, J. A., and T. J. Mitchison. 1991. Actin microfilaments dynamics in locomoting cells. *Nature (Lond.).* 352:126–131.
Theriot, J. A., and T. J. Mitchison. 1992. Comparison of actin and cell surface dynamics in motile fibroblasts. *J. Cell Biol.* 118:367–377.
Wang, Y.-L. 1985. Exchange of actin subunits at the leading edge of living fibroblasts: possible role of treadmilling. *J. Cell Biol.* 101:597–602.
White, J. G., and G. G. Borisy. 1983. On the mechanisms of cytokinesis in animal cells. *J. Theor. Biol.* 101:289–316.
White, J. G., and A. A. Hyman. 1987. On the implications of laterally mobile cortical tension elements for cytokinesis. *In* Biomechanics of Cell Division. NATO ASI Series. N. Akkas, editor. Plenum Publishing Corp., New York. 79–96.
Wolpert, L. 1960. The mechanics and mechanism of cleavage. *Int. Rev. Cytol.* 10:163–216.